Repumping ground-state population in a coherently driven atomic resonance

Asif Sinay*, Moshe Shuker, Ofer Firstenberg, Amnon Fisher, Amit Ben-Kish, Jeff Steinhauer

Department of Physics, Technion-Israel institute of technology, Israel
**asif.sinay@gmail.com*

Abstract: We experimentally demonstrate an optical pumping technique to pump a dilute rubidium vapor into the $m_F = 0$ ground states. The technique utilizes selection rules that forbid the excitation of the $m_F = 0$ states by linearly-polarized light. A substantial increase in the transparency contrast of the coherent-population-trapping resonance used for frequency standards is demonstrated.

©2010 Optical Society of America

OCIS codes: (270.1670) Coherent optical effects; (020.3690) Line shapes and shifts.

References and links

1. J. Vanier, "Atomic clocks based on coherent population trapping: a review," Appl. Phys. B **81**(4), 421–442 (2005).
2. E. Arimondo, "Coherent population trapping in laser spectroscopy," Prog. Opt. **35**, 257–354 (1996).
3. J. Vanier, M. W. Levine, D. Janssen, and M. Delaney, "Contrast and linewidth of the coherent population trapping transmission hyperfine resonance line in 87Rb: Effect of optical pumping," PRA **67**(6), 065801 (2003).
4. Y. Y. Jau, A. B. Post, N. N. Kuzma, A. M. Braun, M. V. Romalis, and W. Happer, in Proceedings of the 2003 IEEE Int. Freq. Control Symp. & PDA Exhibition Jointly with the 17th Euro. Freq. and Time Forum, 33 (2003).
5. Y. Y. Jau, A. B. Post, N. N. Kuzma, A. M. Braun, M. V. Romalis, and W. Happer, "Intense, narrow atomic-clock resonances," Phys. Rev. Lett. **92**(11), 110801 (2004).
6. Y. Y. Jau, E. Miron, A. B. Post, N. N. Kuzma, and W. Happer, "Push-pull optical pumping of pure superposition states," Phys. Rev. Lett. **93**(16), 160802 (2004).
7. T. Zanon, S. Tremine, S. Guerandel, E. De Clercq, D. Holleville, N. Dimarcq, and A. Clairon, "Observation of Raman–Ramsey Fringes With Optical CPT Pulses," IEEE Trans. Instrum. Meas. **54**(2), 776–779 (2005).
8. M. Rosenbluh, V. Shah, S. Knappe, and J. Kitching, "Differentially detected coherent population trapping resonances excited by orthogonally polarized laser fields," Opt. Express **14**(15), 6588–6594 (2006).
9. A. V. Taichenachev, V. I. Yudin, V. L. Velichansky, S. V. Kargapoltsev, R. Wynands, J. Kitching, and L. Hollberg, "High-contrast dark resonances on the D1 line of alkali metals in the field of counterpropagating waves," JETP Lett. **80**(4), 236 (2004).
10. S. V. Kargapoltsev, J. Kitching, L. Hollberg, A. V. Taichenachev, V. L. Velichansky, and V. I. Yudin, "High-contrast dark resonance in σ+–σ- optical field," Laser Phys. Lett. **1**(10), 495–499 (2004).
11. M. Zhu, "High Contrast Signal in a Coherent Population Trapping Based Atomic Frequency Standard Application", M. Zhu, in Proceedings of the 2003 IEEE International Frequency Control Symposium & PDA Exhibition Jointly with the 17th European Frequency and Time Forum, 16 (2003).
12. A. V. Taichenachev, V. I. Yudin, V. L. Velichansky, and S. A. Zibrov, "On the Unique Possibility of Significantly Increasing the Contrast of Dark Resonances on the D1 Line of 87Rb," JETP Lett. **82**(7), 398–403 (2005).
13. E. E. Mikhailov, T. Horrom, N. Belcher, and I. Novikova, "Performance of a prototype atomic clock based on lin||lin coherent population trapping resonances in Rb atomic vapor", arXiv:0910.5881 (2009).
14. G. Kazakov, I. Mazets, Yu. Rozhdestvensky, G. Mileti, J. Delporte, and B. Matisov, "High-contrast dark resonance on D2-line of 87Rb in a vapor cell with different directions of the pump-probe waves," Eur. Phys. J. D **35**(3), 445–448 (2005).
15. D. A. Steck, Rubidium 87 D Line Data, Theoretical Division (T-8), MS B285 Los Alamos National Laboratory Los Alamos, NM 87545 25 September 2001 (revision 1.6, 14 October 2003).
16. W. Happer, "Optical Pumping," Rev. Mod. Phys. **44**(2), 169–249 (1972).
17. C. Cohen-Tannoudji, J. Dupont-Roc, and G. Grynberg, "Atom-Photon Interactions: Basic Processes and Applications", 1998.
18. M. Shuker, O. Firstenberg, Y. Sagi, A. Ben-kish, N. Davidson, and A. Ron, "Ramsey-like measurement of the decoherence rate between Zeeman sublevels," Phys. Rev. A **78**(6), 063818 (2008).
19. S. Knappe, J. Kitching, L. Hollberg, and R. Wynands, "Temperature dependence of coherent population trapping resonances," Appl. Phys. B **74**(3), 217–222 (2002).
20. I. Novikova, Y. Xiao, D. F. Phillips, and R. L. Walsworth, "EIT and diffusion of atomic coherence," J. Mod. Opt. **52**(16), 2381–2390 (2005).

#127648 - $15.00 USD Received 27 Apr 2010; revised 19 Jun 2010; accepted 24 Jun 2010; published 19 Aug 2010
(C) 2010 OSA

1. Introduction

A well-studied technique to implement an all-optical atomic frequency standard utilizes a coherent population trapping (CPT) resonance [1,2] within the ground-state of an alkali atom. The clock transition is defined between two magnetically-insensitive $m_F = 0$ levels of the ground state. The short-term frequency stability of the clock is determined by the width and the amplitude of the transparency resonance and by the accompanied noise. The amplitude of the CPT resonance is proportional to the atomic population within the clock transition, and hence it is desirable to increase the population fraction in the relevant $m_F = 0$ states. At thermal equilibrium, the atoms are equally distributed among all possible ground-state sub-levels, and only a small fraction participates in the clock transition. Moreover, the common approach of using a circularly polarized light optically pumps most of the atoms into the highly polarized spin states [3], further reducing the population in the $m_F = 0$ states. While this pumping is useful for end-state schemes, which utilize the absence of spin-exchange relaxation in highly polarized states [4,5], it is harmful to the $m_F = 0$ CPT resonance.

Several techniques have been proposed to increase the CPT contrast by reducing the effect of pumping to highly polarized states. Most of these introduce an additional laser field, with the orthogonal circular polarization, that effectively pumps the atoms back to the central $m_F = 0$ levels, while maintaining most of the CPT coherence. The destructive interference between the induced coherence of the two circular polarizations can be circumvented by temporarily alternating the left and right polarizations [6]; by inducing an appropriate phase delay (lin⊥lin), either with co-propagating beams [7,8] or with a counter-propagating configuration [9,10]; or utilizing the AC stark shift [11]. An alternative approach utilizes the four $m_F = \pm 1$ Zeeman states, instead of the $m_F = 0$, using a symmetric configuration of left and right circular polarization (lin‖lin) [12,13].

Here we experimentally demonstrate a technique to improve the CPT contrast, by pumping the atoms to the $m_F = 0$ levels with a π-polarized beam (Figs. 1a and 1b). The technique, theoretically suggested by Kazakov *et al.* [14], exploits the forbidden optical transitions $(F = 1, m_F = 0) \rightarrow (F' = 1, m_F = 0)$ and $(F = 2, m_F = 0) \rightarrow (F' = 2, m_F = 0)$, which have a vanishing dipole matrix elements [15]. Using a modulated π-polarized pumping beam, all ground levels except the two $m_F = 0$ are repumped, leading to increased population in the clock transition (depopulation optical pumping [16]). We further investigate additional effects of the repump beam, such as broadening and off-resonance pumping. In section 2, we describe a theoretical model for CPT in a multi-level atom, incorporating the four optical modes and all the relevant atomic levels. In addition to the CPT process, the model describes population pumping to the end state, ground-state depolarization, and re-pumping of population to the $m_F = 0$ levels. In section 3, we describe the experimental setup. In section 4, we detail the experimental results showing the predicted increase in contrast, due to the repump beam, along with a broadening of the CPT line. Finally, we conclude our work in section 5 and discuss the results.

2. Model system

The full 16-level structure of the D1 transition of ^{87}Rb is depicted in Fig. 1a. The common model for CPT with σ^+ light, describing CPT in the $m_F = 0$ resonance, reduces the atomic structure to a 3-level Λ-system. These levels represent the two ground 'clock states', $(F = 1, m_F = 0)$ and $(F = 2, m_F = 0)$, and one excited state, e.g., $(F' = 2, m_F = 1)$. These are denoted as $|1\rangle$, $|2\rangle$, and $|3\rangle$, respectively, and are coupled by two σ^+-polarized electromagnetic fields. However, in order to allow for more elaborated processes, such as optical pumping, a more detailed model is required. Our model includes four additional states as illustrated in Fig. 1c. To account for the ground-state depopulation and for the σ^+ optical pumping, we represent the $m_F \neq 0$ states in the ground manifold by the effective state $|4\rangle$, denoted as the 'trap state'. To incorporate the re-pumping action of the modulated repump beam, we represent the $m_F \neq 0$ states in the excited levels by the effective state $|5\rangle$, denoted as the 'π-excited state'. State $|4\rangle$ is coupled to state $|5\rangle$ by a π-polarized electromagnetic field. To account for off-resonance

#127648 - $15.00 USD Received 27 Apr 2010; revised 19 Jun 2010; accepted 24 Jun 2010; published 19 Aug 2010
(C) 2010 OSA

pumping of the repump beam, as explained later, we represent the excited $m_F = 0$ states, ($F' = 1$, $m_F = 0$) and ($F' = 2$, $m_F = 0$), by two effective states, $|6\rangle$ and $|7\rangle$, denoted as the 'off-resonance pumping states'. Due to selection rules for the π-polarization, state $|1\rangle$ is decoupled from state $|6\rangle$, and state $|2\rangle$ is decoupled from state $|7\rangle$. Therefore, in our model, the π-polarized fields off-resonantly couple states $|1\rangle$ to $|7\rangle$ and $|2\rangle$ to $|6\rangle$. The excited states, $|3\rangle$, $|5\rangle$, $|6\rangle$, and $|7\rangle$, may spontaneously decay to all the lower levels in accordance with selection rules, and the ground states, $|1\rangle$, $|2\rangle$, and $|4\rangle$, exhibit standard population transfer and decoherence.

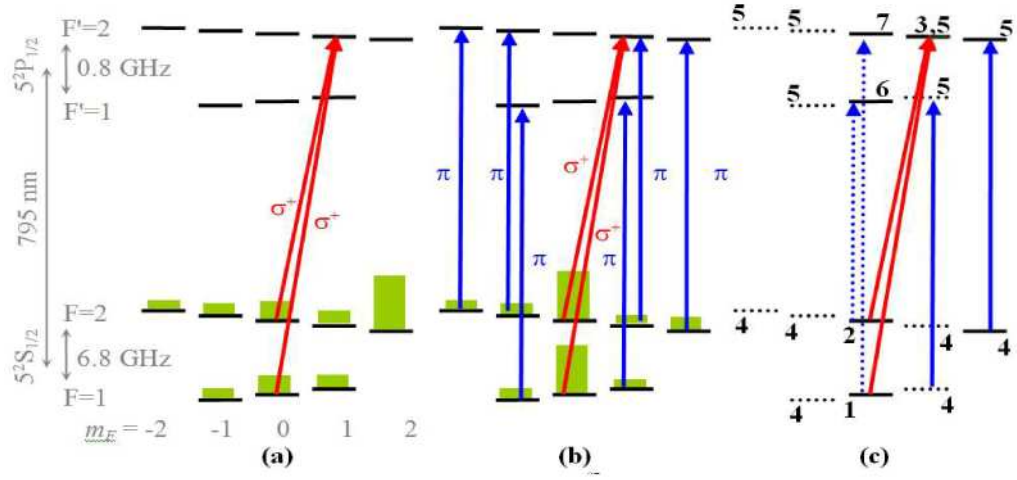

Fig. 1. (Color online) Energy levels diagram for the CPT clock in ^{87}Rb D1 line. The green bars are an illustration of the expected population distribution. (a) Without the repump beam: the σ^+-beam create the CPT resonance while pumping the population towards the end state ($m_F = 2$). (b) With the modulated repump beam: the π transitions ($F = 1$, $m_F = 0$) → ($F' = 1$, $m_F = 0$) and ($F = 2$, $m_F = 0$) → ($F' = 2$, $m_F = 0$) are forbidden, and thus the repump beam repumps the population to the $m_F = 0$ states. (c) The effective states and allowed transitions in the numerical model are marked: the CPT states (1, 2, and 3), the 'trap state' (4), the 'π-excited state' (5), and the 'off-resonance pumping states' (6 and 7). The dashed arrows represent the off-resonant π-excitations.

The model Hamiltonian is given by

$$H = \hbar\sum_{i=1}^{7}\omega_i |i\rangle\langle i| - \hbar\sum_{\{i,j\}}\left[\Omega_{ij}e^{-i(\omega_i-\omega_j+\Delta_{ij})t}|i\rangle\langle j| + H.c.\right], \quad (1)$$

where $\hbar\omega_i$ are the energies of the states, and Ω_{ij} are the Rabi frequencies for each of the relevant transitions $j \to i$. Δ_{ij} are the individual one-photon detunings, and we set $\Delta_{ij}=0$ for transitions $1\to3$, $2\to3$, and $4\to5$, and $\Delta_{ij}\neq0$ for $1\to7$ and $2\to6$. The steady-state solution of the system, in terms of a density operator, is obtained numerically by solving the Master equation $(d/dt)\rho = [H,\rho]/(i\hbar) + L\rho$, yielding the absorption coefficients for the various fields and the population distribution in the ground state [17]. The non-Hamiltonian decay processes are introduced using the Lindblad formalism, with

$$L\rho = \sum_m \gamma_m \left(C_m \rho C_m^+ - \tfrac{1}{2}\rho C_m^+ C_m - \tfrac{1}{2} C_m^+ C_m \rho\right), \quad (2)$$

where C_m are the Lindblad operators, and γ_m are the associated decay rates. Depolarization (population transfer) and decoherence within the ground state are described, respectively, by Lindblad operators of the form $C_{\text{dep.}}=|i\rangle\langle j|$ [with (j=1,2,4)→(i=1,2,4)] and $C_{\text{gound .dec.}}=|i\rangle\langle i|$ [with (i=1,2,4)]. Spontaneous emission is described by $C_{\text{spon.}}=|i\rangle\langle j|$ [with (j=3,5,6,7)→(i=1,2,4),

#127648 - $15.00 USD Received 27 Apr 2010; revised 19 Jun 2010; accepted 24 Jun 2010; published 19 Aug 2010
(C) 2010 OSA

except the forbidden transitions (7→2) and (6→1)]. Decoherence of the optical transitions, taking into account the homogenous pressure-broadening due to the buffer gas, is incorporated with $C_{\text{opt.dec.}}=|i\rangle\langle i|$ [with (i=3,5,6,7)].

The cell temperature and thus the atomic density were constant in all experiments and have been determined from absorption measurements. Some of the dipole matrix-elements and the decay rates in the model are effective parameters and thus required calibration. In practice, we have set them according to relevant known values of the 16-level system [18], and only used the Rabi frequency of the repump beam as a fit parameter. Also, we have calibrated an effective frequency detuning for the off-resonant π-transitions from the relevant experiments, as detailed below.

3. Experimental setup

The experimental setup is depicted in Fig. 2 (left). A vertical-cavity surface-emitting laser diode (VCSEL) is stabilized to the *D1* transition of ^{87}Rb (~795 nm). The VCSEL is current-modulated at 3.417 GHz, and the –1, +1 sidebands are tuned to the $F = 2 \rightarrow F' = 2$, $F = 1 \rightarrow F' = 2$ transitions, respectively (CPT-VCSEL in Fig. 2). The polarization is set to right-circular by a polarizing beam-splitter and a quarter-wave plate. The beam passes through a cross-shaped vapor cell along the z-direction, and the transmitted intensity is measured with a photo-diode. A second VCSEL (repump-VCSEL) is current modulated at ~3 GHz, and its –1, +1 sidebands are tuned to the $F = 2 \rightarrow F' = 2$, $F = 1 \rightarrow F' = 1$ transitions, respectively. The repump-VCSEL is set to linear polarization parallel to the z-direction (π-polarization), and passes the vapor cell in perpendicular to the CPT beam. The intensity of both beams is controlled by neutral-density filters.

The cross-shaped vapor cell (Fig. 2, right) contains isotopically pure ^{87}Rb and 10 Torr of nitrogen buffer gas. The dimensions of the cell are 18 mm length, along the z-direction, and 6 mm diameter. Due to technical limitations, the overlap of the repump beam along the optical path of the CPT beam is limited to 6 mm. Therefore, only one third of the path within the cell is directly repumped (see Fig. 2). The temperature of the cell is controlled using electrical heaters (glass with ITO coating), setting the rubidium vapor density to $n = 7\text{x}10^{10}$atoms/cc. The resulting small-signal transparency is about 40%, providing the optimal conditions for a CPT clock [19]. A four-layered magnetic shield is used to isolate the cell from the earth magnetic field. Three sets of Helmholtz coils are used to set a small magnetic field, B_z = 20mG, along the z-direction, and to eliminate the residual magnetic field in the perpendicular plane. The CPT spectrum is obtained by shutting-down the electrical heaters and scanning the frequency of the RF oscillator, which modulates the CPT-VCSEL current, around the CPT clock-transition. The scanning rate is sufficiently slow, so that the steady-state spectrum is obtained.

#127648 - $15.00 USD Received 27 Apr 2010; revised 19 Jun 2010; accepted 24 Jun 2010; published 19 Aug 2010
(C) 2010 OSA

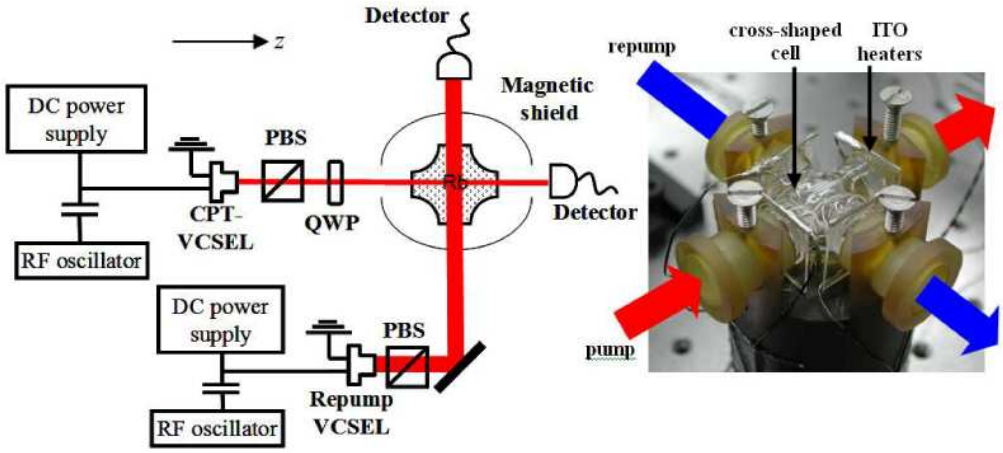

Fig. 2. Experimental setup. Left: VCSEL – vertical cavity surface emitting laser; PBS – polarizing beam-splitter; QWP – ¼-wave plate (Not shown: three sets of Helmholtz coils within the magnetic shield). Right: The cross-shaped glass vapor cell with Indium-Tin-Oxide (ITO) heaters pressed against its four facets.

4. Results

We study the CPT spectrum of our experimental system while applying the repump beam. For five different CPT-VCSEL intensities, we vary the repump-VCSEL intensity and measure the CPT resonance. Each CPT line is fitted to a Voigt profile, and its full width at half maximum (FWHM) and contrast (the ratio between the CPT resonance amplitude and its background) are inferred. Figure 3 (left) depicts the measured CPT contrast of the spectrum versus the repump-VCSEL intensities for the five different CPT-VCSEL intensities.

When the intensity of the CPT-VCSEL is weak, the pumping to high m_F states is small, and the positive effect of the repump is negligible, as shown by the black curve. As the intensity of the CPT-VCSEL is increased, a larger fraction of the atoms is pumped to higher m_F states, and the repump beam is more effective, bringing back more atoms to the $m_F = 0$ state and increasing the CPT contrast, as shown by the red curve. The effectiveness of the repump beam depends also on its intensity. Obviously at low intensities, the repump effect is small, and it increases with the intensity. However at larger intensities, the improvement in the contrast diminishes, and eventually the contrast begins to drop. This is attributed mostly to the off-resonant pumping from the m_F=0 states, as predicted by our numerical model, and possibly also to small imperfections in the polarization of the repump beam. The solid lines in Fig. 3 are the results of our numerical model, showing a good agreement with the experimental results. Figure 3 (right) depicts the measured CPT linewidth (FWHM) versus the repump-VCSEL intensity at five different CPT-VCSEL intensities. The CPT lines broaden with the laser intensity due to power broadening.

#127648 - $15.00 USD Received 27 Apr 2010; revised 19 Jun 2010; accepted 24 Jun 2010; published 19 Aug 2010
(C) 2010 OSA

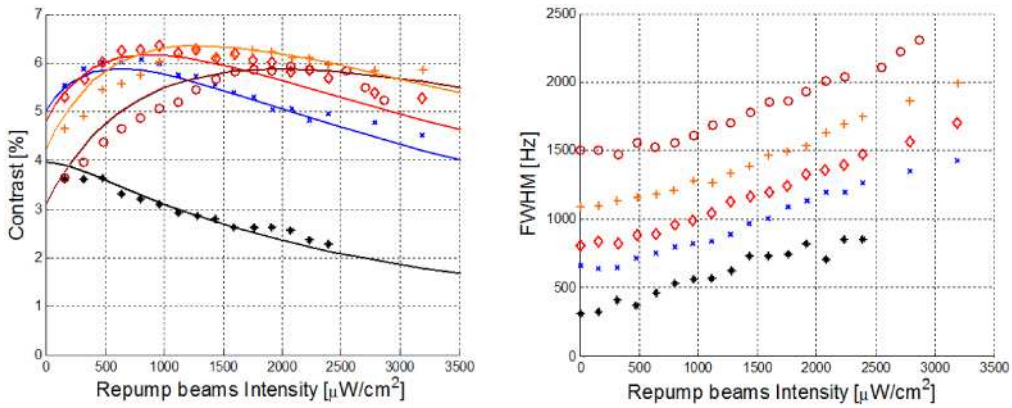

Fig. 3. (Color online) The CPT contrast (left) and FWHM (right) as a function of the repump-VCSEL intensity at different CPT-VCSEL intensities (* Black 1440μW/cm2, x Blue 4320μW/cm2, ◊ Red 5760μW/cm2, + Orange 8640μW/cm2, ○ Brown 12960μW/cm2). The lines are our model's results.

A second set of measurements was devoted to verifying the effectiveness of the repump, by studying the CPT spectrum *without* applying the repump beam. Figure 4 depicts the measured properties of the CPT spectrum at various laser intensities. The CPT linewidth increases linearly with the laser intensity due to power broadening. The CPT contrast initially increases with the laser intensity, but then decreases as the population is pumped out of the clock transition into the high m_F states [3], in good agreement with our numerical model. This phenomenon poses a fundamental limit on the maximal contrast that can be obtained in this CPT apparatus and limits the possible accuracy of CPT based frequency standards.

The maximal increase in contrast achieved using the repump beam, for different CPT-VCSEL intensities, is also plotted in Fig. 4 (along with the associated FWHM). It is important to note that, due to technical limitations in the current apparatus, the repump beam is applied to only one third of the length of the cell, limiting the effectiveness of the repumping method.

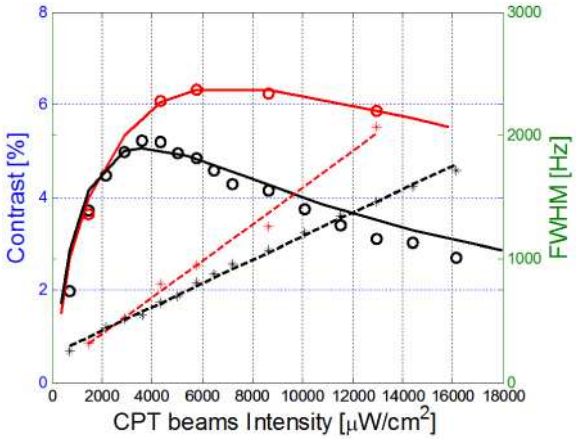

Fig. 4. (Color online) The CPT contrast (circles) and the CPT FWHM (asterisks) without the repump beam (black) and with the repump beam (red). For each intensity of the CPT beam, the maximal contrast, obtained by scanning the repump-beam intensity, is shown. The solid lines are model results.

To obtain the best frequency stability, it is important to maximize the contrast and to minimize the linewidth [1]. Therefore, in order to use this optical pumping technique to substantially improve the short-term frequency stability, it is necessary to pump the atoms without increasing the CPT linewidth due to power broadening. One option is to time-

#127648 - $15.00 USD Received 27 Apr 2010; revised 19 Jun 2010; accepted 24 Jun 2010; published 19 Aug 2010
(C) 2010 OSA

alternate the repump beam, and to perform the CPT measurement when the repump beam is off. Another possibility is to apply the repump beam in the vicinity of the CPT beam, but with minimal spatial overlap. In the latter case, the repumping effect will be obtained utilizing the diffusion of atoms in the cell [20].

The contrast observed at the optimum operating point of the system is ~6.1% using the repump beam, instead of 5% without the repump beam. For an arrangement of maximal spatial overlap of the two beams, our numerical model predicts a contrast of about 20%, demonstrating an improvement of a factor of 4.

5. Conclusion

We have demonstrated an optical pumping technique to increase the contrast of CPT-based frequency standards utilizing two additional optical modes (a modulated repump beam). The improvement of the CPT contrast was studied for a wide range of CPT and repump beams intensities. A major drawback of this pumping method is the power broadening of the CPT resonance associated with the repump beam. This limitation may be prevented by turning off the repump beam just before making the measurements or by applying them in the near vicinity of the CPT beam, with minimal spatial overlap. We estimate that by using an optimal setup, the contrast may be improved by up to a factor of four.

Acknowledgements

We thank Yoav Erlich, Igal Levi and Kosta Kogan for technical support. This work is partially supported by the fund for encouragement of research in the Technion and by the DDRND.

#127648 - $15.00 USD Received 27 Apr 2010; revised 19 Jun 2010; accepted 24 Jun 2010; published 19 Aug 2010
(C) 2010 OSA